Journal of the European Ceramic Society **12** (1993) 297–308

Pressureless (Liquid-Phase) Sintering of X-Phase and Mullite/X-Phase Powders

C. C. Anya & A. Hendry

University of Strathclyde, Department of Metallurgy and Engineering Materials, Colville Building, Glasgow G1 1XN, UK

(Received 12 February 1993; revised version received 26 March 1993; accepted 26 April 1993)

Abstract

X-Phase and mullite/X-phase composite powders, derived by carbothermal reduction and nitriding of kaolinitic clays, have been respectively sintered to 100 and 95% theoretical density by pressure-less sintering. Powders with lower proportions of mullite gave higher relative density values. Optimal densification could only be achieved by attention to a combination of factors such as powder composition, type of embedding powder, two-step sintering, temperature and time.

With the aid of X-ray diffraction, scanning and transmission electron microscopy, it is shown that in mullite/X-phase powders, further transformation of mullite to X-phase occurs during sintering (in a N_2 atmosphere), because of reduction in the sample by CO (in the sintering gas) formed by the oxidation of carbon from the graphite linings of the furnace. X-Phase nucleates directly from mullite. Kinetics of the process revealed that it is controlled by a liquid phase. X-Phase in both powder and sintered forms is triclinic (a = 9·68, b = 8·56, c = 11·21 Å, α = 91·4, β = 124·4 and γ = 99·2°) and (pseudo) orthorhombic (a = 9·66, b = 2·84, and c = 11·17 Å) when analysed by X-ray and electron diffraction, respectively.

X-Phase und Mullit/X-Phase Verbundpulver, hergestellt durch karbothermische Reduktion und Nitrierung von kaolitischem Ton, wurden auf eine Dichte von 100 bzw. 95% der theoretischen Dichte druckgesintert. Pulver mit einem geringeren Mullitgehalt ergaben eine relativ höhere Dichte. Eine optimale Verdichtung konnte nur unter Beachtung verschiedener Faktoren wie Pulverzusammensetzung, Art des Einbettpulvers, zweistufiges Sintern, Temperatur und Zeit erreicht werden.

Mit Hilfe von Röntgenbeugung, Raster- und Transmissionselektronenmikroskopie konnte gezeigt werden, daß in Mullit/X-Phase Pulvern eine weitere Transformation von Mullit in X-Phase während des Sinterns (in einer N_2 Atmosphäre) stattfindet. Verursacht wird dies durch die Reduktion der Proben durch CO (im Sintergas), das durch die Oxidation des Kohlenstoffs der Graphitauskleidung des Ofens entsteht. X-Phase bildet sich direkt aus Mullit. Aus der Kinetik des Prozesses geht hervor, daß er durch eine flüssige Phase kontrolliert wird. Sowohl im Pulver als auch in den gesinterten Formen liegt die X-Phase in trikliner (a = 9·68, b = 8·56, c = 11·21 Å, α = 91·4, β = 124·4 und γ = 99·2°) bzw. (pseudo) orthorombischer (a = 9·66, b = 2·84 und c = 11·17 Å) Form vor, wenn die Charakterisierung durch Röntgenbeugung bzw. Elektronenbeugung erfolgt.

Des poudres de phase X et des poudres composites phase X/mullite, obtenues par réduction carbothermale et nitruration d'argiles kaolinitiques, ont été frittées sans pression, respectivement jusqu'à 100 et 95% de la densité théorique. Une densification optimale ne pu seulement être obtenue qu'en prenant attention à une série de facteurs tels que la composition de la poudre, le type de lit de frittage, un frittage en deux étapes, la température et la durée.

A l'aide de la diffraction RX, des microscopies électroniques à balayage et à transmission, les auteurs ont montré que dans les poudres mullite/phase X, une transformation de la mullite en phase X se produit durant le frittage (dans une atmosphere d'azote) en raison de la réduction de l'échantillon par le CO (dans le gaz de frittage) formé par l'oxydation du carbone utilisé dans la construction du four. La phase X croît par nucléation directement à partir de la mullite. Les cinétiques mesurées révèlent que ce processus est contrôlé par une phase liquide. La phase X, en poudre et dans le fritté, est triclinique (a = 9·68, b = 8·56,

Journal of the European Ceramic Society 0955-2219/93/$6.00

c = 11·21 Å, α = 91·4, β = 124·4 et γ = 99·2°) et pseudo-orthorombique (a = 9·66, b = 2·84 et c = 11·17 Å), selon que l'analyse est effectuée par diffraction RX ou d'électrons.

1 Introduction

The flexural strength of mullite, relative to other engineering ceramics, does not appreciably deteriorate at high temperatures up to about 1500°C.[1] However, a silica-rich phase (glass) that is often associated with mullite constitutes a major limitation on its use as a structural engineering material at such high temperatures. This is because the possibility of creep deformation above the softening point of the glass, normally far below the melting point of mullite, is very much enhanced. If the amount of the silica-rich phase can be reduced, this will improve the overall mechanical properties of mullite.

One way of reducing the silica phase, and thus improving the mechanical properties of mullite, is by a carbothermal reduction and nitriding process, whereby some of the mullite is transformed to X-phase by reaction with the silica phase. Thus,

$$3(3Al_2O_3 . 2SiO_2) + 6SiO_2 + 12CO + 4N_2 \rightarrow Si_{12}Al_{18}O_{39}N_8 + 12CO_2 \quad (1)$$

However, work by Yamagishi *et al.*[2] suggests that such an improvement is limited to only about 15% X-phase in mullite. An earlier work by Yamagishi *et al.*,[3] in which mullite/X-phase composites were made by reacting mullite with up to 15 vol.% additions of β-sialon ($z = 2$), revealed that the sintering process by which the mullite/X-phase composite products were made gave heterogeneous products between the surface and the bulk of the sample, depending on the nature of the immediate atmosphere around the sample. Thus situations where the samples were not embedded in a powder led to the formation of X-phase, mullite and α-Al_2O_3 in the bulk but no X-phase on the surface. Where the samples were embedded in a powder (mullite), α-Al_2O_3 was eliminated by vacuum sintering, but was still present in a nitrogen atmosphere and again no X-phase was formed at the surface. The formation of X-phase was achieved by the transformation of mullite in intimate contact with β′-sialon. In this work[2,3] mechanical properties, particularly toughness, degrade with deterioration of bulk density, which in turn occurs as the formation of more X-phase (transformation) takes place.

When materials transform, depending on the compatibility of the new and old structures, structural stresses may build up, and most often these structural stresses adversely affect mechanical properties such as toughness. Given that the results in the work of Yamagishi *et al.*[2] demonstrate the considerable extent of the transformation and the paucity of reports on the mechanical properties of monolithic X-phase, it was decided to investigate the sintering behaviour of powders of X-phase (no transformation) and mullite/X-phase (with transformation). This paper only reports on the bulk density property. A discussion, however, is made of the likely effect of the density results on mechanical behaviour.

2 Materials and Experimental

X-Phase and mullite/X-phase powders were produced by carbothermal reduction and nitriding of kaolinitic clays (compositions are given in Table 1) according to schedules reported[4,5] by the present authors.

A cold isostatic press was used to pack the powders for sintering in graphite-lined furnaces in nitrogen atmosphere. Two types of bedding powder, β′-sialon ($z = 3$, hereafter designated as 401) and a mixture (by weight) of 38·5% SiO_2, 38·5% Si_3N_4 and 23% BN (henceforth referred to as M553) were used. The presence of CO in the exhaust gas was monitored with an infra-red gas analyser.

The shrinkage of sintered pellets was evaluated and used for kinetic studies. The average grain sizes of the sintered pellets were obtained using an image analyser (Olympus Q2M). Some sintered pellets were sectioned, ground to 40 μm and then thinned with an ion beam for transmission electron microscopy (TEM). The distribution of phases in the mullite/X-phase composite samples was more effectively studied using the scanning electron microscopy (SEM), to which an energy dispersive X-ray analyser (EDAX) was attached. Bulk densities were determined using Archimedes' principle (immersion of samples in water).

Table 1. Compositions of the kaolinitic clay[4]

ECC[a] (Grade D) clay			
Chemical	*(wt%)*	*Mineral*	*(%)*
SiO_2	46·88	Kaolinite	85
Al_2O_3	37·65	Mica	12
Fe_2O_3	0·88	Feldspar	3
TiO_2	0·09	—	—
CaO	0·03	—	—
MgO	0·13	—	—
K_2O	1·60	—	—
Na_2O	0·21	—	—
Loss on ignition	12·45	—	—

[a] ECC = English China Clay company, the suppliers of the clay.

3 Results and Discussions

3.1 Sintering process

3.1.1 Further transformation of mullite to X-phase; evolution of CO

Figure 1 is the observed evolution of CO against time of sintering of 60% mullite–40% X-phase powder which resulted in a 40% mullite–60% X-phase composite product after sintering. The numbers in the figure are the temperatures in degrees Celsius recorded at specific times. Two experiments were carried out; the first one was at 1560°C for 1 h, with a first step at about 1375°C for 30 min (Fig. 1(a)), while the second experiment was at 1560°C for 1 h, but with only one step (Fig. 1(b)). The fact to be noted from these figures is that the peak volume of evolved CO is within the most probable temperature range (about 1400–1560°C) for X-phase transformation.

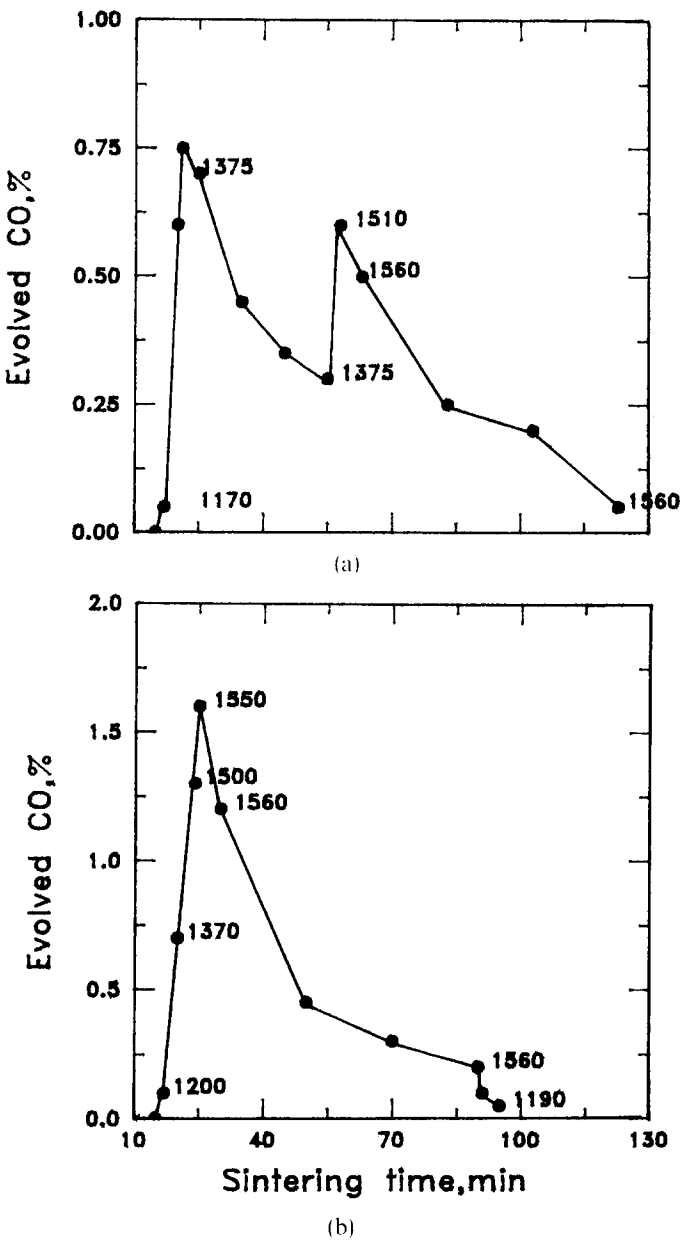

Fig. 1. Evolution of CO versus sintering time. Figures in the graph are the temperatures (in °C) at these times. (a) With 2 steps; (b) with 1 step.

In an earlier work[5] the present authors suggested that the CO evolution results from the oxidation of unburnt carbon from the carbothermal powder production stage. This is not the case. In the present report, the furnace was heated up without any charge and under the same conditions as when a pellet was present. For both cases, CO evolution took place and was exactly as in Fig. 1. Thus, it was concluded that the evolution of CO during sintering is due to the oxidation of carbon from graphite linings of the furnace by residual oxygen from the furnace atmosphere. The CO then diffuses into the sample where more X-phase is formed according to eqn (1). Further confirmation that the evolved CO from graphite linings was responsible for the transformation of mullite to X-phase (in the presence of nitrogen) during the process was obtained by sintering the samples in a furnace devoid of any carbon in any form under similar conditions. There was no transformation of mullite to X-phase.

The transformation of mullite to X-phase during sintering is very fast and can be extensive; for instance, a carbothermally produced powder of about 30% mullite in X-phase, after sintering for only 2 min, results in 100% X-phase (detectable constituents by XRD).

3.1.2 Effect of two-step sintering, bedding powder and powder composition on densification

In a preliminary sintering experiment, it was observed that sintering in two steps reduced weight loss and porosity of sintered samples. This was thought to be due to elimination of the bulk of the evolved CO_2 less vigorously and outside the transformation temperature range. From Fig. 1, it is evident that sintering with only one step leads to more than twice the average specific volume of evolved CO compared to that obtained using a two-step sintering technique.

The need for two-step sintering increases if an optimal choice of bedding powder is not made. When M553 was used as a bedding powder, there was no weight loss at all for both composite mullite/X-phase and X-phase powders. However, using sialon 401, there was an appreciable weight loss. In comparison, the weight loss was less in situations with two sintering steps as against those with one sintering step. The former gave an average weight loss of 5 and 4% for X-phase and X-phase/mullite composites respectively. One-step sintering led to a weight loss of about 12% for X-phase and the same 4% for X-phase/mullite powders.

With M553 a greater extent of pore closure was observed, unlike in the cases with sialon 401, where

pore closure was less effective. For the 95 and 100% theoretical densities that were achieved in the present work for X-phase/mullite composite powder and X-phase sialon, respectively, marginally higher sintering temperatures were attainable using the M553 bedding powder (Fig. 2). This is because the M553 bed leads to a higher partial pressure of SiO. This permits the use of a higher sintering temperature, which then leads to more closure of pores and hence to a better densification.

Yamagishi *et al.*[3] made a similar observation about the effect of bedding powder in relation to the improvement of sintered products. They found that using mullite as a bedding powder for sintering mullite/β-sialon (to yield a mullite/X-phase composite product) eliminated the formation of α-Al_2O_3, although they still had a difference in composition between the bulk (where X-phase was formed) and the surface that had only mullite. The β-sialon totally decomposed. The partial pressure of SiO has been suggested[6] to be responsible for the effect of bedding powder on sintered products. Thus, the generation of a pressure of SiO from the bedding powder higher than that of the sample being sintered guarantees that volatilization of the latter is drastically reduced or even eliminated. It is therefore clear that sialon 401 (β') being of a lower eq% oxygen value than either X- or mullite phase in the SiO_2–Al_2O_3–Si_3N_4–AlN phase diagram generates a lower pressure of SiO than would either of the two phases. However, with M553 the SiO pressure will be higher than that of X-phase and similar to that of mullite from the sample being sintered.

Although for similar compositions the sintering temperature difference for the two types of bedding powder is only about 25°C at the most (Fig. 2), the significance of this rather small difference becomes clear if the microstructures of a sample of 100% X-phase powder sintered at 1680°C (Fig. 3(a)) and at the optimal temperature of 1665°C (Fig. 3(b)) in M553 are compared. Note the difference in porosity adduced by an increase of only 15°C over the optimal sintering temperature. Also the effect of using a sintering temperature less than the optimal by 15°C leads to about 5 and 3·5% reduction of bulk density in the sintered X-phase and composite mullite/X-phase powders respectively. Hence, it can be said that the temperature range for optimal sintering of X-phase, or composites containing it, is very narrow, and therefore demands stringent sintering conditions. Variation of bulk density with sintering temperature for 60% mullite/40% X-phase powder sintered for 1 h, after which it transformed

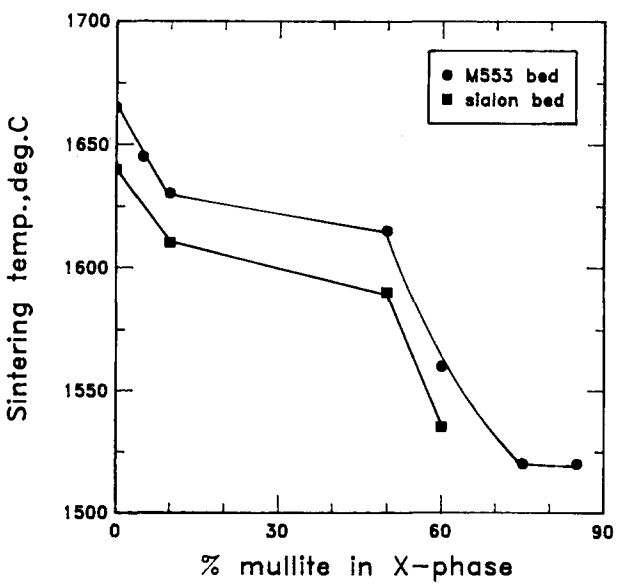

Fig. 2. Sintering temperature (°C) versus mullite concentration in X-phase (for starting powders) for different bedding powders. With mullite concentrations $\leq 30\%$, the sintered product consists of only X-phase as the crystalline constituent.

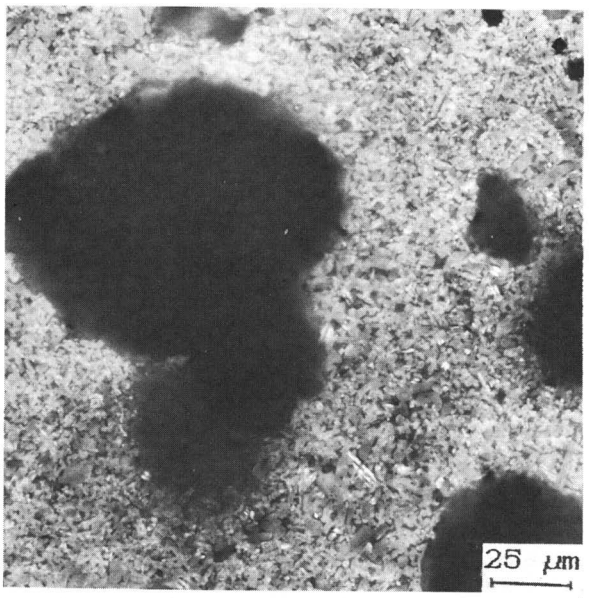

(a)

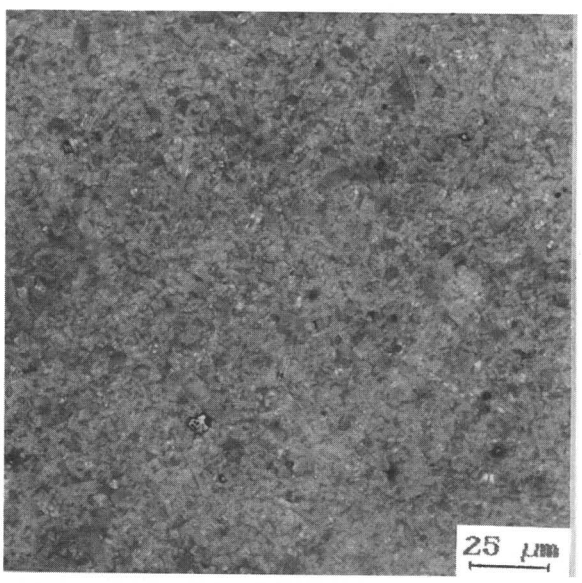

(b)

Fig. 3. Effect of sintering temperature on the structure X-phase: (a) sintered at 1680°C; (b) sintered at an optimal temperature of 1665°C.

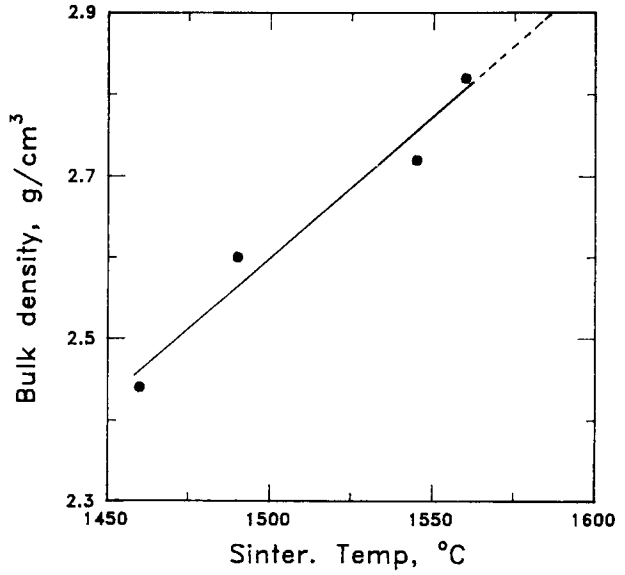

Fig. 4. Bulk density of a 40% mullite/60% X-phase composite product sintered for 1 h in the M553 bed. The initial composition of the powder was 60% mullite/40% X-phase.

to 60% X-phase/40% mullite, is shown in Fig. 4. At each of these sintering temperatures, the final product was the same.

The overall positive effect of two-step sintering and the use of the M553 bedding powder led to better bulk density values (Fig. 5). In this figure it should be noted that the mullite concentration refers to the composition of powders before sintering, and that only those compositions with the concentration of mullite above 30% will produce mullite/X-phase sintered products. This is because at concentrations $\leq 30\%$, the mullite completely transforms to X-phase.

Worthy of note in Figs 2 and 5 are two facts: firstly, the optimal sintering temperature depends on the relative composition of the two phases, to the

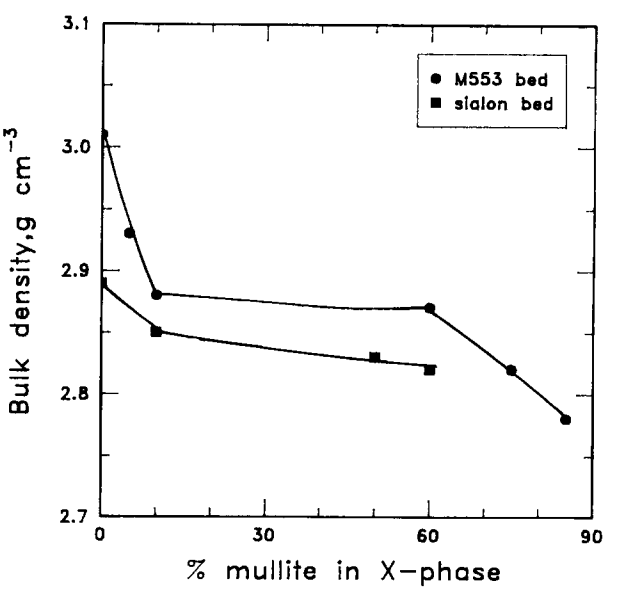

Fig. 5. Bulk density of sintered products at optimal temperatures for 1 h versus mutual proportions of mullite and X-phase in starting powders for different bedding powders.

effect that higher mullite contents lead to lower sintering temperatures, as observed in the present work (Fig. 2). This observation may partly explain the high porosity of an X-phase/10% mullite sample sintered at 1740°C for 1 h in the work of Wills *et al.*[7] Thus the presence of mullite in their sample should have necessitated a lower sintering temperature. The second fact is that a lower mullite content (formed *in situ*) leads to an improvement of the bulk density of sintered samples (Fig. 5). The improvement is such that with 100% X-powder, the theoretical density of 3·01 g cm^{-3} of the phase[8] is achieved by pressureless sintering.

3.1.3 Kinetics of composite mullite/X-phase and X-phase sintering

On transforming kaolinite to mullite or X-phase (of formula $Si_{12}Al_{18}O_{39}N_8$) during the carbothermal powder production stage, the following are the general equations:

$$3(2SiO_2 . Al_2O_3 . 2H_2O) \rightarrow (3Al_2O_3 . 2SiO_2) + 4SiO_2 + 6H_2O \quad (2)$$

$$9(2SiO_2 . Al_2O_3 . 2H_2O) + 12C + 4N_2 \rightarrow Si_{12}Al_{18}O_{39}N_8 + 6SiO_2 + 12CO + 18H_2O \quad (3)$$

Whereas the amount of silica associated with mullite is 36 wt%, that associated with X-phase is about 18·8 wt%. So it may be proposed that for carbothermally produced composite powders of both phases, the increase in relative densities and the change in optimal sintering temperatures as the amount of mullite present decreased must be related to the amount of silica-rich phase present. A strong support for this proposition as it relates to the effect of this silica-rich phase on the density and optimal sintering temperatures was found in a parallel experiment, in which carbothermally derived X-phase was mixed with commercially pure Baikalox mullite and sintered. Thus, in a sintered product of 40% mullite/60% X-phase (initial compositions of both phases being produced carbothermally *in situ*), a bulk density of 2·87 g cm^{-3} was obtained after 90 min at 1560°C in an M553 bed. However, in a similar composition, in which only X-phase was carbothermally produced and the mullite was pure, under similar processing conditions, a bulk density of 3·01 g cm^{-3} was obtained at 1620°C. Therefore, if these changes to the density and the sintering temperatures of carbothermally derived composite powders of mullite and X-phase are related to the silica-rich phase, which could be a source of liquid phase, then the kinetics should follow the usual trend of liquid-phase sintering as enunciated by Kingery.[9] The kinetics of the sintering process were therefore studied. For this purpose, one-step sintering was

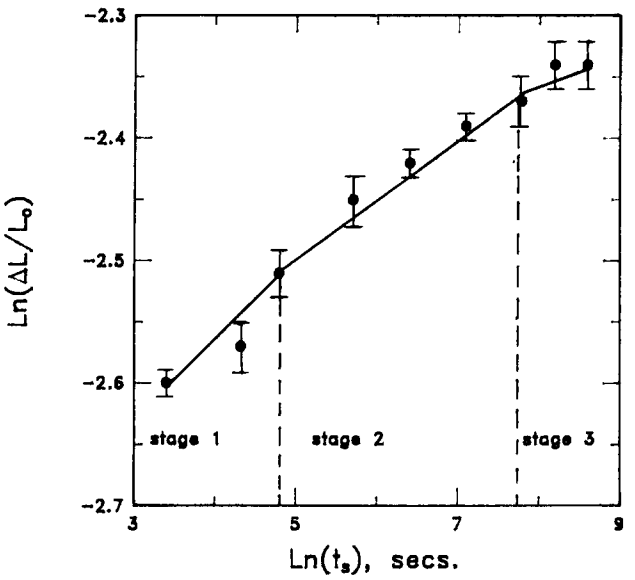

Fig. 6. Relative shrinkage versus sintering time for 40% mullite/60% X-phase sintered product.

adopted, and the 60% mullite/40% X-phase powder, which, after sintering in the M553 bedding powder at 1560°C produced 40% mullite/60% X-phase (detected crystalline phases), was used.

In Fig. 6 is the relative shrinkage ($\Delta L/L_0$) of the samples plotted against time (t). A very fast and high densification was observed for these samples. Within as little as 10 min, a bulk density of 90·6% of the theoretical density was achieved. The theoretical densities of X-phase and mullite were respectively taken to be 3·01 and 3·16 g cm^{-3}.

It can be seen in Fig. 6 that the curve may be interpreted as a three-stage liquid-phase sintering process. A more vivid distinction of the stages can be found in Fig. 7, a graph of rate of densification, $d\Delta L/dt$, against sintering time, t. Thus the first stage of variable kinetics associated with particle rearrangement[9] leaves no definite trend. The second (reprecipitation; process control) stage starts from around the 5th minute in the figure, which is marked by a definite trend of slowing densification rate till around the 42nd minute. The start of the third stage is marked by a constant densification rate from around this 42nd minute, before it starts to drop again and drops ultimately to zero.

With regard to the second stage (the reprecipitation or process control stage, according to Kingery,[9] diffusion becomes the limiting process if the relative shrinkage, $\Delta L/L_0$, follows a relationship of the type:

$$\Delta L/L_0 = P(r)^{-4/3}(t)^{1/3} \quad (4)$$

If, however, the phase (solid–liquid) boundary reaction is the limiting factor, $\Delta L/L_0$ should follow the relationship:

$$\Delta L/L_0 = Q(r)^{-1}(t)^{1/2} \quad (5)$$

where P and Q are constants, r is the average grain size and t is the sintering time. Though relations (4) and (5) are specifically for spherical particles, they still hold for prismatic particles such as those in the present study (shown later in this work). This is because, as suggested by Kingery,[9] shrinkage due to the edges of the prismatic particles obtains only at the very early stages of the sintering process; moreover, the difference which may arise from the prismatic nature of the grains is only reflected in the constant terms, P and Q. The slope of this second stage (Fig. 6) was found to be $0{\cdot}04 \pm 0{\cdot}001$.

The average grain sizes of the sintered samples obtained within the second stage were plotted against sintering time and the plot is shown in Fig. 8 as a linear variation of $\ln(r)$ versus $\ln(t_s)$. The microstructure of the mullite/X-phase composite products was of polygonal X-phase and acicular mullite, which showed an average aspect ratio of $4{\cdot}7 \pm 0{\cdot}4$. Hence, it was considered that the acicular-

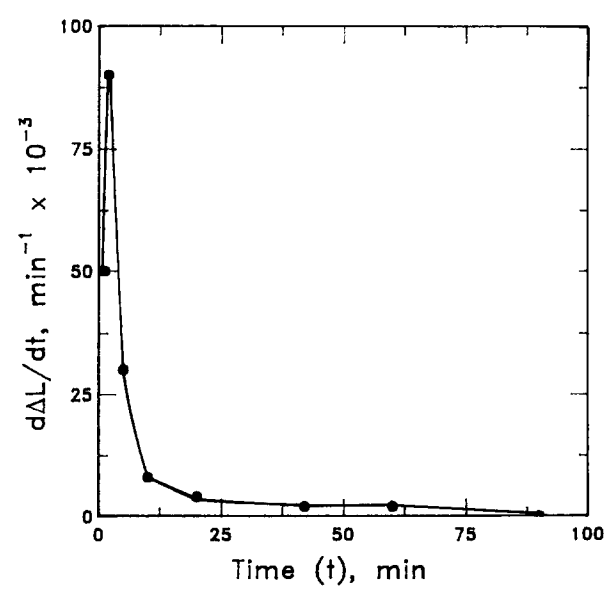

Fig. 7. Densification rate versus sintering time for 40% mullite/60% X-phase sintered product.

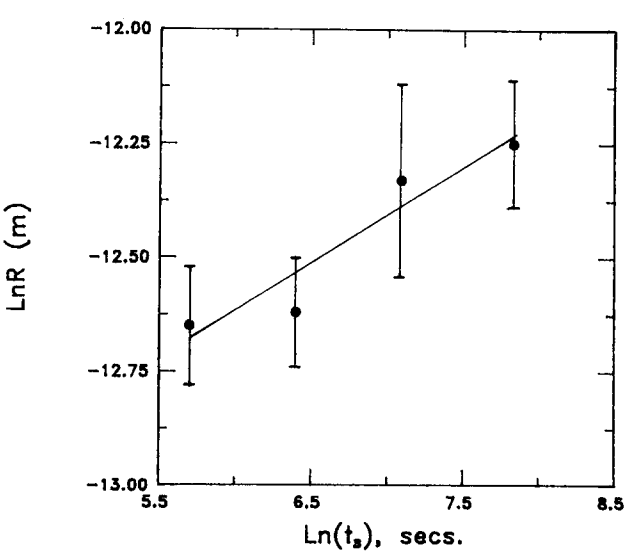

Fig. 8. Evolution of grain size with time of sintering.

ity of mullite is of no consequence to the evolution of grain size with time during the sintering process. The slope of Fig. 8 is $0{\cdot}21 \pm 0{\cdot}01$. Thus, the following relationship can be written:

$$\ln(r) = S + 0{\cdot}21 \ln(t)$$

or

$$r = S(t)^{0{\cdot}21} \tag{6}$$

where S is a constant. A similar relationship was used[10] to describe grain growth controlled by either grain boundary impurities or intergranular phase. Introducing this experimental variation of r with t into eqns (4) and (5), respectively

$$\Delta L/L_0 = PS^{0{\cdot}21}(t)^{0{\cdot}05} \tag{7}$$

$$\Delta L/L_0 = QS^{0{\cdot}21}(t)^{0{\cdot}29} \tag{8}$$

Since P, Q and S are constants, eqns (7) and (8) can respectively be written as $\Delta L/L_0 = B(t)^{0{\cdot}05}$ and $\Delta L/L_0 = A(t)^{0{\cdot}29}$. Considering that the evolution of shrinkage with time for the second stage showed a slope of $0{\cdot}04 \pm 0{\cdot}001$, it is rational to conclude that

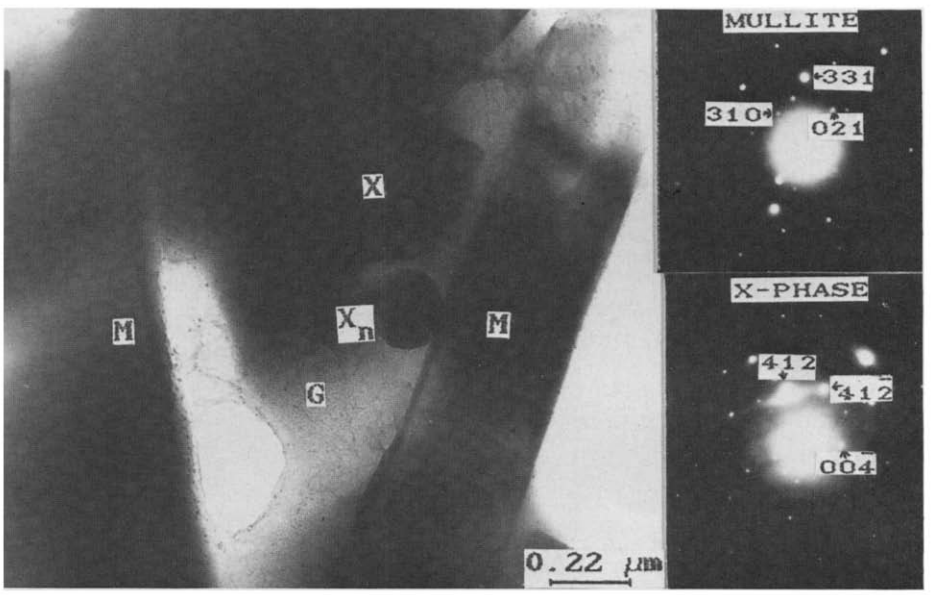

(a)

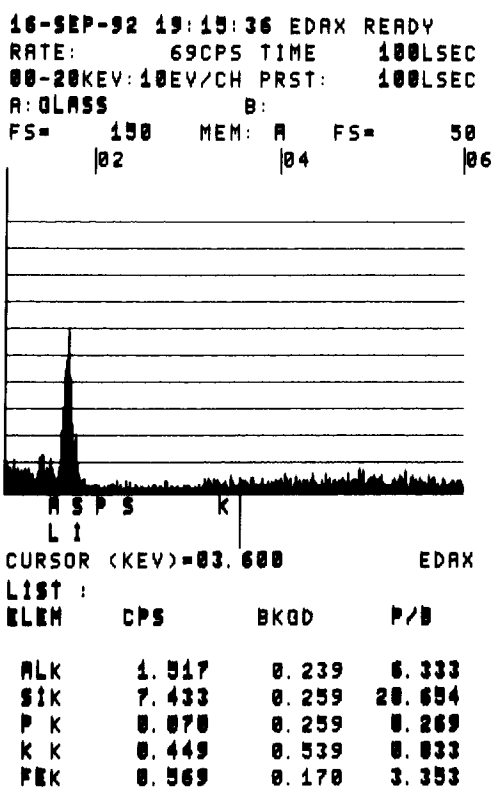

(b)

Fig. 9. (a) TEM micrograph showing the presence of a silica-rich phase (G), into which a grain of X-phase (X_n) nucleated from a mullite (M) grain is growing. Note the perfect contact between the nucleated grain of X-phase and the mullite needle. Inset are the electron diffraction patterns (DP) of mullite and X-phase. (b) TEM EDAX analysis of the silica-rich phase, from which its composition is estimated to be about (by weight) 78% SiO_2, 16% Al_2O_3, 6% FeO and traces of K_2O.

the limiting factor is diffusion, since the deduced slope of 0·05 is closer (than 0·29) to 0·04.

Thus the sintering process can be considered to be controlled by the liquid of a silica-rich phase. In Fig. 9(a) is a TEM micrograph showing a grain of X-phase (marked X_n) nucleating from mullite and growing into the silica-rich phase. Inset are the electron diffraction patterns of the respective phases. The electron diffraction (ED) pattern of the silica-rich phase suggests that it is amorphous (glassy). This is responsible for the background ring pattern exhibited by the ED of the X-phase grain. In Fig. 9(b) is an example of the most common spectra of the ten TEM EDAX analyses carried out on the silica-rich phase. Iron is the principal non-volatilizable impurity (Table 1) of the kaolinitic clay used to produce the X- and mullite phases. Hence, it can be assumed that at the sintering temperatures used in this work, the silica-rich phase consists of SiO_2, FeO (the most stable form of the oxides of iron at these temperatures) and Al_2O_3. Correlating the EDAX results with the details of the SiO_2–FeO–Al_2O_3 ternary diagram,[11] the phase has a solidus temperature of about 1300°C and a liquidus temperature of about 1600°C. Thus, at the sintering temperature of 1560°C, a large volume of liquid is already present. In situations where the amount of this liquid phase is excessive, such as cases with a high amount of mullite, the optimal sintering temperature must remain relatively low to obtain satisfactory densification. Even then, a high amount of the glassy phase would always lead to a lower density relative to the composites with a reduced amount of the glassy phase. This exaplains why the sintered product of the carbothermal powders, as already discussed, showed a lower density (even at the optimal sintering temperature) relative to that shown by a mixture of carbothermally produced X-phase with Baikalox commercially pure mullite.

4 Structure of Sintered X-Phase—Distribution of X- and Mullite Phases in their Sintered Products

4.1 Structure of sintered X-phase

It was shown[4] that carbothermally produced X-phase, when analysed by XRD methods, in agreement with the work of Thompson & Korgul,[8] is triclinic with $a = 9{\cdot}68$, $b = 8{\cdot}56$, $c = 11{\cdot}21$ Å, $\alpha = 91{\cdot}4$, $\beta = 124{\cdot}4$ and $\gamma = 99{\cdot}2°$. In the same report,[4]

Table 2. Indexing parameters of X-phase[a] observed in TEM

Number	*Remarks*	d_1d_2 (*deg.*)	d_1d_3 (*deg.*)	d_1 (Å)	d_2 (Å)	d_3(Å)
1	Observed	110	66	2·68	2·09	2·01
	Calculated	111·1	65·8	2·68	2·09	2·05
	(*hkl*)			$\bar{1}0\bar{4}$	311	$21\bar{3}$
2	Observed	61	27	2·62	2·09	1·34
	Calculated	62·3	27·1	2·65	2·09	1·36
	(*hkl*)			$\bar{1}1\bar{1}$	311	220
3	Observed	110	72	1·84	1·20	1·18
	Calculated	108·9	71	1·82	1·18	1·18
	(*hkl*)			$4\bar{1}\bar{1}$	324	713
4	Observed	65	37	2·40	2·04	1·31
	Calculated	66·3	36·2	2·39	2·03	1·31
	(*hkl*)			211	205	416
5	Observed	76	48	3·68	2·40	1·84
	Calculated	76·4	47·6	3·65	2·39	1·82
	(*hkl*)			202	$21\bar{1}$	411
6	Observed	91	54	3·78	2·73	2·23
	Calculated	90	53·8	3·72	2·72	2·20
	(*hkl*)			003	110	113
7	Observed	69	34	2·06	2·03	1·25
	Calculated	69	34·9	2·09	2·05	1·26
	(*hkl*)			311	$\bar{2}13$	124
8	Observed	81	47	2·16	1·72	1·26
	Calculated	81·8	46·3	2·18	1·75	1·28
	(*hkl*)			$\bar{1}05$	412	317
9	Observed	95	62	3·68	2·26	2·01
	Calculated	95·08	62·2	3·65	2·24	1·99
	(*hkl*)			202	$\bar{2}12$	014
10	Observed	94	55	2·76	1·84	1·60
	Calculated	94·6	54·9	2·75	1·83	1·58
	(*hkl*)			$01\bar{1}$	502	511
11	Observed	108	71	2·79	1·75	1·75
	Calculated	108·2	71·8	2·79	1·75	1·75
	(*hkl*)			004	412	$41\bar{2}$

[a] Considered as orthorhombic, with $a = 9{\cdot}66$, $b = 2{\cdot}84$, $c = 11{\cdot}17$ Å.

however, it was also shown that samples of X-phase are (pseudo) orthorhombic when analysed by the TEM method, using linear lattice parameters suggested by Thompson & Korgul:[8] $a = 9{\cdot}66$, $b = 2{\cdot}84$ and $c = 11{\cdot}17$ Å for high X-phase.

They[8] obtained the phase by slow cooling from a melt and suggested that both the low and high X-phase forms are triclinic, with the latter, in addition to the linear lattice parameters given previously, also having angular parameters of $\alpha = 90$, $\beta = 124{\cdot}4$ and $\gamma = 98{\cdot}5°$. Similarly, other workers,[12,13] analysing sintered X-phase by the TEM method, suggested that the phase is triclinic. So it was thought that the discrepancy between these results,[8,12,13] which identified both types of X-phase as triclinic, and those of the work[4] by the present authors which identified high X-phase to be (pseudo) orthorhombic, may be attributable to the methods through which the phase was obtained. However, it was suggested[4] that this discrepancy is due to the complex nature of X-phase and the complementary roles of TEM and XRD techniques. It was decided therefore to study the structure of sintered X-phase and compare it with that of carbothermally obtained X-phase powder.

The results revealed that just like the carbothermally obtained form, with the same lattice parameters, sintered X-phase is triclinic and (pseudo) orthorhombic when analysed by XRD and TEM techniques respectively. However, the reflection intensities in the XRD pattern of sintered X-phase show a slight variation from those of its form obtained carbothermally. It was observed that reflections such as 201 ($d = 4{\cdot}717$ Å, $2\theta = 18{\cdot}8°$) and 103 ($d = 2{\cdot}427$ Å, $2\theta = 37°$) disappear, while a reflection such as 211 ($d = 4{\cdot}433$ Å, $2\theta = 20°$) becomes very, very weak.

This variation in intensity may be the result of rearrangement of particle morphology during the sintering process, which could alter the relative intensities of planes. The parameters of some of the indexed ED patterns of sintered X-phase are entered in Table 2. In Fig. 10(a) is a TEM bright-field micrograph of a grain of X-phase. The indexing parameters of Fig. 10(c) are entered in Table 2 as numbers 1 and 2. Note the heavily twinned structure of the phase.

4.2 Distribution of X- and mullite phases in their sintered products

TEM and SEM studies revealed that the two phases in some cases are interwoven, see Fig. 11(a)–(d). In Fig. 11(a) and (b) mullite needles hold together grains of X-phase. Note the highly faulted grain of X-phase (marked X_n) which nucleated from mullite. Figure 11(c) and (d) show the distribution as revealed by SEM. The constituents were identified

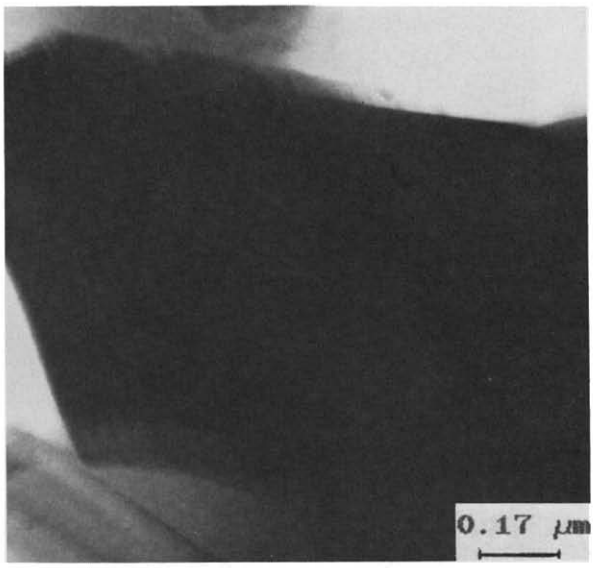

(a)

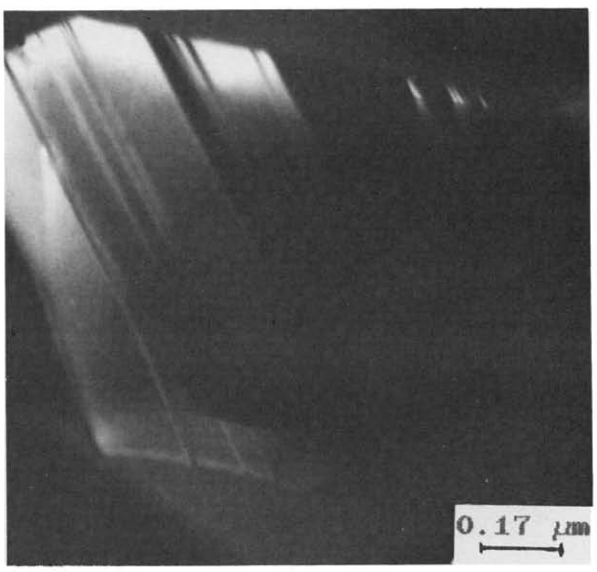

(b)

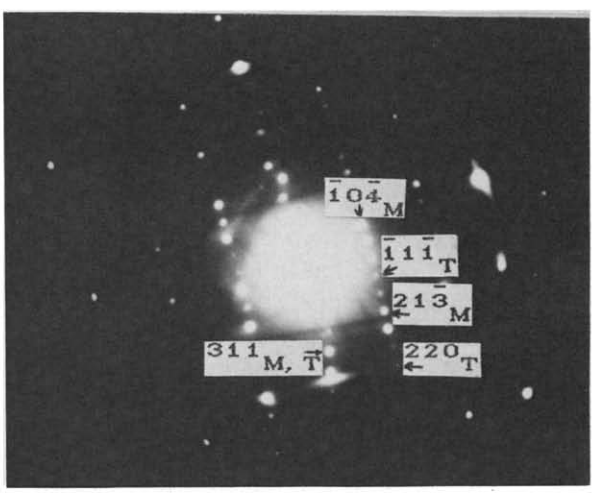

(c)

Fig. 10. TEM micrograph of a grain of X-phase: (a) bright field (BF); (b) dark field (DF); (c) DP; M = matrix; T = twin.

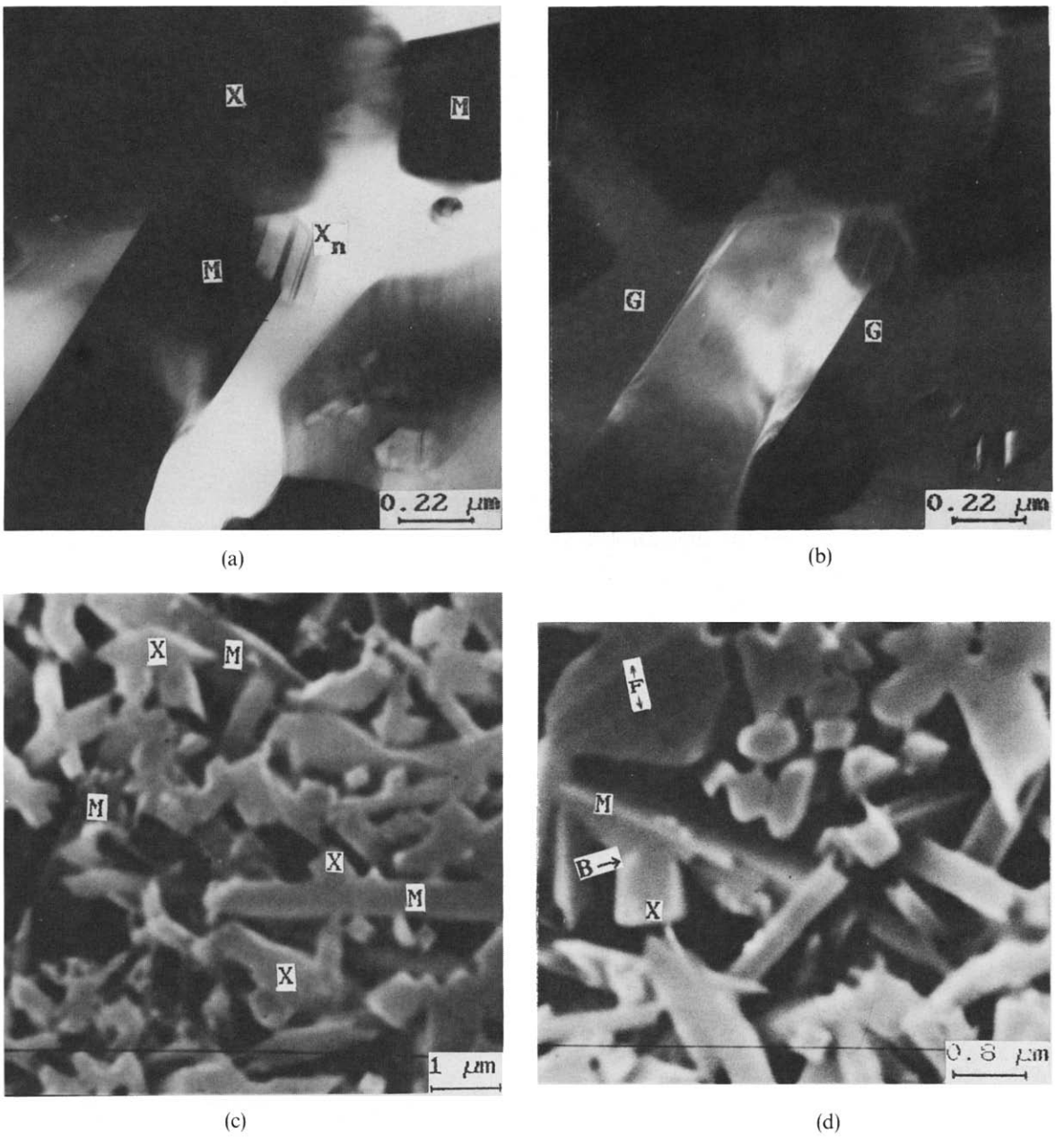

Fig. 11. TEM micrographs (a) (BF) showing the distribution of mullite (M) and X-phase (X); X_n is a nucleated grain of X-phase (note the perfect match between X_n and M, and the relative sizes of X (pre-existing) and X_n (nucleated) grains of X-phase) and (b) (DF) of features in Fig. 11(a) showing clearly the glassy (G) regions; SEM micrographs (c) showing the interwoven nature of the distribution of X- (X) and mullite (M) phases and (d) showing the distribution of X- and mullite phases, perfect contact between the two at regions (for example, B) where the former nucleated from the latter and the relative sizes of a pre-existing faulted grain (F) and a nucleated grain (X) of X-phase; SEM EDAX spectra of (e) mullite and (f) X-phase.

using the EDAX facility attached to the SEM and the respective spectra are shown in Fig. 11(e) and (f). Note also the faults in the large X-phase grain (F) of Fig. 11(d). Another interesting feature in Fig. 11(d) is the relative sizes of X-phase grains in mullite–X-phase sintered products. The smallness of the X-phase grain in contact with mullite at the region marked B suggests that the large-sized X-phase grains (an example being the one marked F) were mostly pre-existing, while the newly formed X-phase grains, precipitated during sintering, are relatively smaller in size. Note also in this figure (Fig. 11(d), B region) that the newly formed grain of X-phase maintains a perfect contact with mullite. A similar observation was made in the TEM, Figs 9 and 11(a) and (b). Yamagishi *et al.*[2] also made a similar observation of the absence of liquid phase between mullite and X-phase in a sintered product of the two.

Using optical microscopy it is not easy to differentiate mullite from X-phase in their sintered composite products. However, it was observed that using carbothermally produced powders, as the mullite content increases, the sintered product colour changes from grey to black. This also could be inferred from the optical micrographs in which the sample containing both phases, Fig. 12(a), appears darker than those containing only X-phase (crystalline phase only), Fig. 12(b).

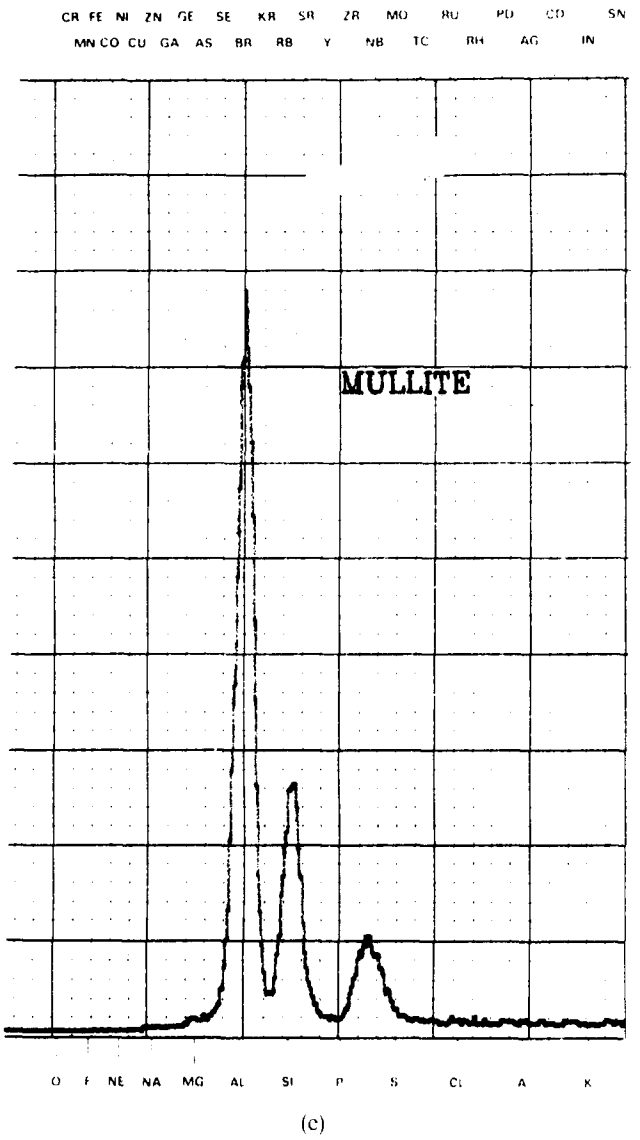

(c)

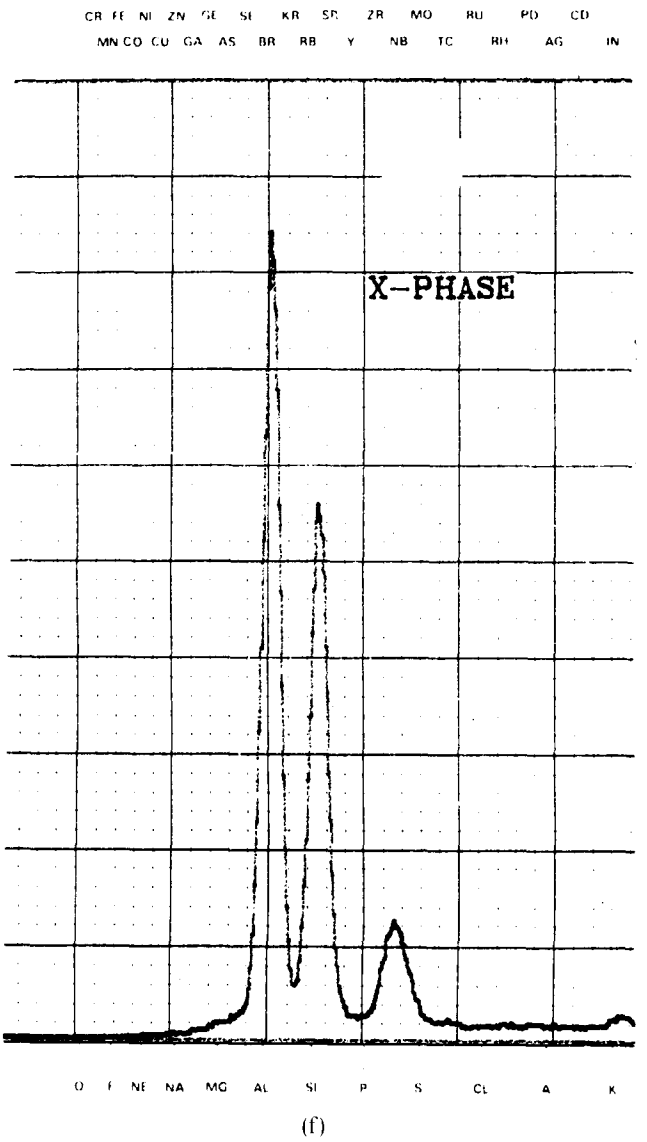

(f)

Fig. 11. *contd.*

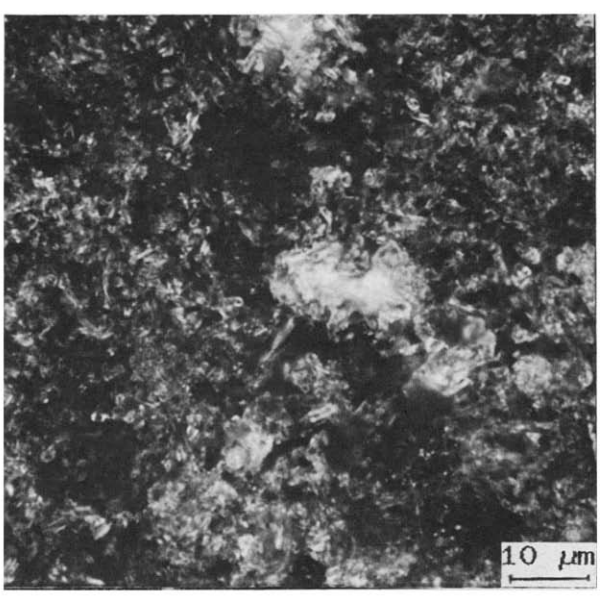

(a)

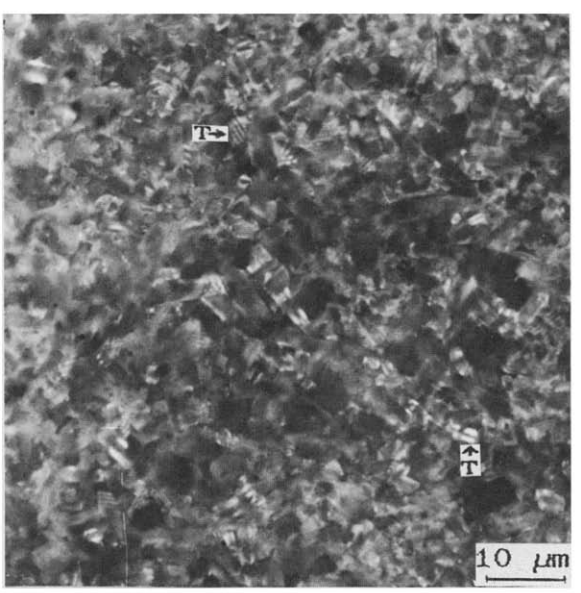

(b)

Fig. 12. Optical micrographs of (a) sintered carbothermally derived mullite/X-phase composite; (b) sintered carbothermally derived X-phase. T = Twins. Note that the sintered composite is darker in colour.

5 Discussion

As mentioned in the Introduction, in the work of Yamagishi *et al.*,[2,3] improvement of bulk density values more often translated into better mechanical properties; however, greater than 5% X-phase in mullite (more transformation) translated into poorer density values.

In the present work, it can be seen that powders with more pre-existing X-phase always had higher density values after sintering (Fig. 5). In other words, whenever less transformation takes place the density values become higher. Since most of the time higher density values translate into better mechanical properties, it is most probable that the transformation process, by deteriorating the density values, could have a similar effect on the mechanical properties.

The melting point of X-phase is estimated[14] to be 1720°C. Yet, using natural precursor raw materials (kaolinitic clays with impurities) it was possible to sinter X-phase to 100% theoretical density at a temperature only 55°C short of its melting point. An attempt to sinter a mullite mixture obtained by calcination of the same kaolin clay, under the same conditions as used in this work and at 1600°C (about 200°C lower than the melting point of mullite) was unsuccessful. It was very porous and no X-phase was formed. Lack of formation of X-phase implies that an intimate contact of mullite with the reducing and nitriding agents is required for X-phase to be formed. The high porosity of the sintered mullite is most probably due to the high content of the silica-rich phase which, as has already been discussed, has a low solidus temperature. Further support to the last statement can also be found in the parallel experiment with X-phase/Baikalox pure mullite, in which both high density and higher sintering temperature were achieved. The high density values achieved for sintered X-phase and the X-phase/Baikalox mullite composite in this work represent a good indicator that if mullite is reinforced with pre-formed X-phase sialon (thereby eliminating transformation), and sintered respecting the stringent conditions imposed by the amount of X-phase, improved mechanical properties of the composites, relative to those of mullite, could be achieved.

6 Conclusions

By pressureless sintering, approximately theoretical density of X-phase sialon is attainable, providing a suitable embedding powder, two-step sintering, optimal temperature and time conditions are adopted. The need for two-step sintering arises from the fact that carbon from graphite linings of the sintering furnace react with oxygen from the furnace atmosphere to form CO. A first step lower temperature sintering reduces the risk of vigorous evolution of gases during sintering.

For both powder and sintered samples, when analysed by XRD and TEM techniques, the X-phase is respectively triclinic and (pseudo) orthorhombic.

Higher density values were obtained in mullite/X-phase composites where transformation was severely reduced or non-existent during sintering. To this end, it is better to avoid such transformations by sintering relatively pure mullite mixed with pre-produced X-phase sialon.

Acknowledgements

Financial support under the BRITE-EURAM programme (contract number, Breu-0064-EDB) is acknowledged. The authors are also grateful for extensive discussion of the mullite/X-phase system with colleagues at the Technical University of Denmark (J. Engell, C. Daugaard) and at CRIBC, Mons, Belgium (F. Cambier, D. Libert).

References

1. Mah, T. & Mazdiyasni, K. S., Mechanical properties of mullite. *J. Am. Ceram. Soc.*, **66**(10) (1983) 699–703.
2. Yamagishi, C., Yoshida, H., Kamaika, H., Asaumi, J. & Miyata, N., Microstructures and mechanical properties of mullite–sialon composites. *J. Japan. Soc. Powder Metall.* (Abstract, Figures and Tables in English), **37**(2) (1990) 187–90.
3. Yamagishi, C., Yoshida, H., Kamaika, H., Asaumi, J. & Miyata, N., Fabrication of mullite–sialon composites. *J. Japan. Soc. Powder Metall.*, **37**(2) (1990) 182–6.
4. Anya, C. C. & Hendry, A., Stoichiometry and crystal structure of X-phase sialon. *J. Eur. Ceram. Soc.*, **10**(2) (1992) 65–74.
5. Anya, C. C. & Hendry, A., Production of X-phase and X-phase/mullite ceramic powders. In *Conf. Proc. Engineering Ceramics: Fabrications, Science and Technology*, 18–20 December 1991, Manchester, UK. ed. D. P. Thompson (Institute of Materials, London). *Brit. Cer. Proc.* **50** (1993) 19–29. Institute of Ceramics. In the press.
6. Edress, H. J., Pressureless sintering of β'-sialon. MSc Thesis, University of Strathclyde, Glasgow, UK, 1987.
7. Wills, R. R., Stewart, R. W. & Wimmer, J. M., Effect of composition and X-phase on the intrinsic properties of reaction-sintered sialon. *Ceram. Bull.*, **56**(2) (1977) 194–203.
8. Thompson, D. P. & Korgul, P., Sialon X-phase. In *2nd NATO ASI Conf. Proc. Progress in Nitrogen Ceramics*, ed. F. L. Riley, M. Nijhoff, Leyden, The Netherlands, 1983, pp. 375–9.
9. Kingery, W. D., Densification during sintering in the presence of a liquid phase I theory. *J. Appl. Phys.*, **30** (1959) 301–6.
10. Mocelin, A., Surfaces and interfaces of ceramics materials, ed. L. C. Dufour, C. Monty & G. Petot-Evras. Kluwer Academic Publishers, Dordrecht, 1989, 485.
11. Levin, E. M., Robbins, C. R. & McMurdie, H. F. (eds), *Phase diagrams for ceramists.* American Ceramic Society, 1964, p. 241, Fig. 696.
12. Zangvil, A., The structure of the X-phase in the Si–Al–O–N alloys. *J. Mat. Sci. Lett.*, **13** (1978) 1370–4.
13. Drew, P. & Lewis, M. H., The microstructures of silicon nitride/alumina ceramics. *J. Mat. Sci.*, **9** (1974) 1833–8.
14. Naik, I. K., Gauckler, L. J. & Tien, T. Y., Solid–liquid equilibria in the system Si_3N_4–AlN–SiO_2–Al_2O_3. *J. Am. Ceram. Soc.*, **61**(7–8) (1978) 332–5.